

Electronic and Structural Properties of Zincblende $B_xIn_{1-x}N$

O. D. Ojuh^{1,2}, N. N. Omehe³, J. O. A Idiodi¹.

1. Physics Department, University of Benin, Benin City, Nigeria.
2. Department of Basic Sciences, Benson Idahosa University, Benin City Nigeria.
3. Western Delta University, Oghara, Delta State Nigeria.

Abstract

We present first-principles calculations of the Structural and electronic properties of zinc blende for different concentrations x of ternary alloy $B_xIn_{1-x}N$. The computational method is based on the pseudopotential method as implemented in the Abinit code. The exchange and correlation energy is described in the local density approximation (LDA) and generalized gradient approximation (GGA). We have investigated the effect of composition on the lattice parameters, bulk modulus and band gap of the zinc blende BN, InN. The results obtained are in a good agreement with experimental and theoretical values concerning the variation of the gaps and crossover from direct to indirect band gap and the bowing parameter.

Keywords: Lattice parameter, bulk modulus, band gap, bowing parameter and Abinit code. .

1. Introduction

Semiconductor materials constitute today basic building blocks of emitters and receivers in cellular, satellite, and fiberglass communication. Among these, the III - nitrides are nowadays widely used by the industry. With respect to “classical” III-V semiconductors, the group-III nitrides semiconductors have attracted much attention in recent years to their great potential for technological applications [1]. The III-nitride semiconductor has received much attention in the past few years since they have important applications in light emitting diodes (LEDs) and short wavelength laser diodes (LD), due mainly to their relatively wide band gap corresponding to the visible region to the near ultraviolet region of the spectrum and high emission efficiency. In addition, bright blue LEDs based on III-nitride semiconductors have already paved the way for full-color displays and for mixing three primary colors to obtain white light for illumination [2]. As well as, the hardness and large bulk modulus make them ideal protective coating materials. It is well-known that the binary zinc-blende BN is an indirect band-gap alloy and the binary zinc-blende in InN is a direct band-gap alloy. Therefore, the ternary zinc-blende $B_xIn_{1-x}N$ alloy with an increase of the boron composition exhibits a

*Corresponding author. Tel.: +2340862614570
E-mail address: dojuh@biu.edu.ng

crossover point where the direct-to-indirect band-gap transition occurs. It is an interesting and important topic to define the crossover point. The emitting wavelength is dependent on the band gap energy of material, and the band gap bowing parameter is important for calculating the band gap energy III-nitride ternary material.

The objective of this work is to investigate the electronic and structural properties of ternary zinc-blende $B_x\text{In}_{1-x}\text{N}$ alloy by using first-principles calculations. The method is based on the pseudopotential method based density functional theory (DFT) in the local density approximation (LDA) and generalized gradient approximation (GGA) as implemented in the Abinit code. The electronic properties, including the band gap energy obtained from band structure, the band gap bowing, and the crossover point of the direct-to-indirect band-gap transition, will be discussed. Furthermore, the structural properties, such as the equilibrium lattice constant, total energy and bulk modulus will be calculate.

2.0 Theory and Computational Procedure

2.1 Total Energy and Functional

Solving the many-body Schrödinger equation allows to obtained many properties of a system of N interacting electrons in the external potential of the nuclei. The Hamiltonian equation is given as:

$$H\psi(r_1, \dots, r_{N_{el}}) = E\psi(r_1, \dots, r_{N_{el}}) \quad 2.1.1$$

While the Schrödinger is state below:

$$H = -\sum_i \hbar^2 / 2M\Delta_i^2 + \sum_i V_{ext}(r_i) + e^2 / 2\sum_{i \neq j} 1 / |r_i - r_j| \quad 2.1.2$$

Where r_i is the position of electron i , Δ_i^2 indicates the Laplacian taken with respect to the coordinate r_i , while $V_{ext}(r_i)$ is the external potential acting on the electrons and depends parametrically on the nuclear positions. In finding a numerical solution for the Schroedinger equation (2.1.1), an efficient method is required. Density Functional Theory (DFT) introduced by Hohenberg and Kohn [20] provides a one-to-one correspondence between the round-state electronic charge density $p(r)$ and the external potential $V_{ext}(r)$. Therefore, since the external potential determines also the many-body wave-function of the ground

state, every physical quantity of the system in its ground state can be expressed as a functional of the electronic charge density. The ground-state total energy of the system plays a prominent role in determining properties of a system, this can be expressed as the expectation value of the Hamiltonian on the ground-state wave-function Ψ_0 . If we express the total energy as a functional of the electronic density then [25, 26],

$$E[p(r)] = \langle \Psi_0 | H | \Psi_0 \rangle = F[p(r)] + \int_V V_{\text{ext}}(r)p(r) d^3 r \quad 2.13$$

Where the integral is performed over the whole volume V of the system. In this equation (2.1.3), $F[p(r)]$ is a universal functional of the density and it is given by the expectation value of the kinetic energy and of electrostatic electron repulsion terms on the ground state. The minimization of the functional $E[p(r)]$ with respect to the electronic density, with the constraint that the number of electrons N_{el} is fixed,

$$\int_V p(r) d^3 r = N_{\text{el}} \quad 2.1.4$$

Gives the ground-state total energy and the electronic density. Kohn and Sham (KS) [21] introduced a new functional by mapping the many-body problem into a non-interacting electrons problem with the same ground-state electronic density because, the exact form of the universal functional $F[p(r)]$ is not known. The new functional can be obtained by recasting the second term in eq. (2.1.3) to the form [20,21]:

$$F[p(r)] = T_0[p(r)] + E_H + E_{\text{XC}}[p(r)] \quad 2.1.5$$

Where the first term is the kinetic energy of a non-interacting electrons system, the second term is the Hartree-like energy term, which accounts for the classical Coulomb interaction of a spatial charge distribution $p(r)$ and the third term represents the exchange-correlation energy [25,26]. The only really unknown quantity is the exchange-correlation energy functional and, in principle, the quality of the solution of the full many-body problem will be only limited by the quality of the approximation. With this new expression for the functional then, the total energy in eq. (2.1.3) becomes:

$$E[p(r)] = \langle \Psi_0 | H | \Psi_0 \rangle = T_0[p(r)] + E_H + E_{\text{XC}}[p(r)] + \int_V V_{\text{ext}}(r)p(r)d^3 r \quad 2.16$$

In order to account for the exchange-correlation energy functional in the above equation, we applied a Local Density Approximation (LDA) and Generalized Gradient Approximation (GGA) [25,26].

2.2 Equation of state and elastic properties

The thermodynamic equation that described and explained state of matter under specified physical conditions is known as equation of state. The equation of state consist of mathematical relationship between two or more state functions such as temperature, pressure and volume. In order to determined the energy-volume relationship which allows us to obtain the equilibrium lattice parameter, we adopt the method proposed by Birch-Murnaghan [27] to fit the data generated by energy-volume calculations;

$$\Delta E(V) = E - E_0 = B V_0 [(V_0/V)^{1/3} B' + (1/3)(1-B') + (V_0/V)^{2/3} B'(B'-1)] \quad 2.2.1$$

Where V_0 is the equilibrium volume at zero pressure, E_0 is the equilibrium energy and B , B' are the bulk modulus and its derivative. Taking the derivative of equ. (2.2.1) we compute the bulk modulus and subsequently obtained the derivative of the bulk modulus.

Our calculations were carried out using the density functional theory with a plane wave basis set as implemented in ABINIT code. [3,4]. The exchange and correlation were treated within the local density approximation (LDA) and generalized gradient approximation (GGA). The self-consistent norm – conserving pseudopotentials were generated using Trouiller- Martins scheme [5] which is included in the Perdew- Wang [6] Scheme as parameterized by Ceperley and Alder [7]. The Brillouin zone was sampled using a 6 x 6 x 6 the Monkhorst- Pack [8] mesh of special K-points. Within the applied self-consistent method, 2984 plane waves were used in this expansion that was determined by a kinetic energy cutoff of 25 Ha. The criterion on the wave function was about 1.0×10^{-10} .

3.0 Results and discussions

3.1 Structural properties

In this work the electronic structure of $B_xIn_{1-x}N$ ternary alloy was calculated using DFT within LDA and GGA methods. In these calculations, the ternary alloy was defined by only specific concentrations of N, In, and B. The calculations have been performed on alloy to introduce the band gaps and lattice constants of the bowing corresponds to the total range of nitrogen, boron and indium concentrations(x) with small increments disregarding the so long computational time.

In ternary semiconductor alloys, the optical bowing is well known phenomenon. This bowing in large band gap of III-V semiconductor has been observed more than thirty years ago by Larach et al [9] on powder material and by Ebina et al[10].

At the first stage of the work, the system is relaxed or optimized with a criterion on the force to 10^{-5} Ha/br to get the lattice constant and the atomic position using the Abinit code. The total energy and the Bulk moduli of the alloy are also calculated for different volumes at each concentration. Figure 3.1 shows Concentration dependence of Lattice constant calculated within DFT-LDA and DFT-GGA and Figure 3.2 shows Concentration dependence of the bulk modulus calculated within DFT-LDA and the DFT-GGA

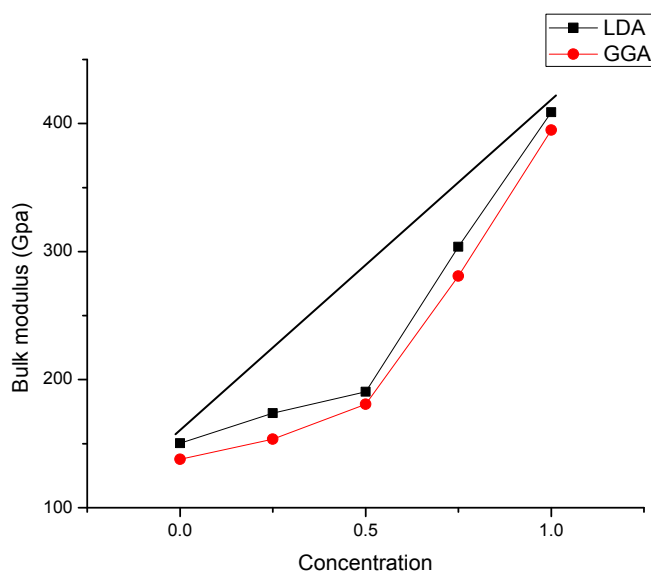


Figure 3.1: Concentration dependence of the bulk modulus calculated within DFT-LDA and the DFT-GGA

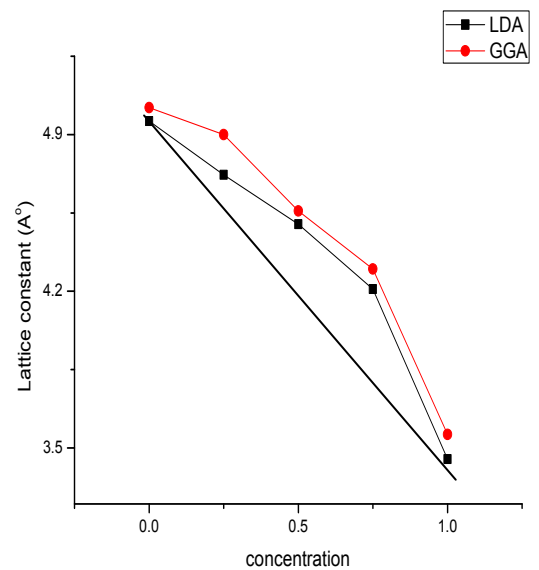


Figure 3.2: Concentration dependence of Lattice constant calculated within DFT-LDA and DFT-GGA

3.2 Electronic properties.

After that, the calculated values of the lattice parameters were used to calculate the band structure for the alloys. The last stage, the energy gaps of the alloys was calculated. Usually, in the treatment of alloys, it is assumed that the atoms are located at the ideal lattice sites and the lattice constant varies linearly with composition x according to the so-called Vegard law[11]

$$a(A_xB_{1-x}C) = xa_{AC} + (1-x)a_{BC}, \quad 3.2.1$$

Where a_{AC} , a_{BC} are the equilibrium lattice constants of the binary compounds AC and BC, respectively, and $a(A_xB_{1-x}C)$ is the alloy lattice constant. However, violation of Vegard's law has been observed in semiconductor alloys both experimentally[12] and theoretical [13,14]. Hence, the lattice constant and energy gap can be written as

$$a(A_xB_{1-x}C) = xa_{AC} + (1-x)a_{BC} - x(1-x)b, \quad 3.2.2$$

and

$$E_g(A_xB_{1-x}C) = xE_{gAC} + (1-x)E_{gBC} - x(1-x)b, \quad 3.2.3$$

Where the quadratic term b is the bowing parameter.

The calculated lattice constant and energy gap of the alloy were fitted to equations 3.2.2 and 3.2.3.

Figure 3.3 – 3.8 show the calculated band structure energies of ternary compounds $B_xIn_{1-x}N$ with x varies from 0.25 to 0.75 using pseudopotential method within LDA and GGA approximation. We obtained an indirect band gap for BN with a value of 4.21 and 4.49eV for LDA and GGA respectively and a direct band gap for InN with a value of 0.00eV. The band gap calculated for the ZB InN using the LDA and GGA describes InN as metallic compound. The ternary $B_xIn_{1-x}N$ shows a direct gap for composition $x= 0.25, 0.5$ and 0.75 . The boron fraction modulates the gap energy from 0.014eV for $x =0.25$ to 3.067 for $x =0.75$. The band gap energy increases considerably with high boron composition x . The $B_{0.75}In_{0.25}N$ is a wide gap semiconductor. The main band gaps are given in table 3 as well as the available theoretical and experimental values. It is clearly seen that the band gaps are on the whole underestimated in comparison

with experiments results. Tables 1 and 2 show the bulk Modulus B in (Gpa) and the theoretical lattice constants in A^0 for $B_xIn_{1-x}N$ in zincblende phase at $x = 0.25, 0.50,$ and 0.75 respectively with other work.

Table 1: *The bulk Modulus B in (Gpa) and the theoretical lattice constants in A^0 for $B_xIn_{1-x}N$ in zincblende phase at $x = 0.25, 0.50,$ and 0.75 respectively with other work*

Composition		LDA	GGA	Other work
$B_{0.25}In_{0.75}N$	$a(A^0)$	4.7200	4.9000	4.213[15]
	B(GPa)	173.75	153.55	173.169[15]
$B_{0.5}In_{0.5}N$	$a(A^0)$	4.5000	4.5590	4.585[15]
	B(GPa)	190.50	180.86	189.638[15]
$B_{0.75}In_{0.25}N$	$a(A^0)$	4.2100	4.3300	4.839[15]
	B(GPa)	303.77	280.88	173.169[15]

Table 2: *The bulk modulus B in (Gpa) and the theoretical lattice constants in A^0 for $B_xIn_{1-x}N$ in zincblende phase at $x=0.25, 0.50,$ and 0.75 respectively.*

Composition		LDA	GGA	Other works/Experiment
InN	$a(A^0)$	4.9600	5.0200	4.920[16] 4.986[17]
	B(GPa)	150.25	137.72	144[18] 137[19]
$B_{0.25}In_{0.75}N$	$a(A^0)$	4.7200	4.9000	
	B(GPa)	173.75	153.55	
$B_{0.5}In_{0.5}N$	$a(A^0)$	4.5000	4.5590	
	B(GPa)	190.50	180.86	
$B_{0.75}In_{0.25}N$	$a(A^0)$	4.2100	4.3300	
	B(GPa)	303.77	280.88	
BN	$a(A^0)$	3.4500	3.5600	3.576[20] 3.615[21,22,23]
	B(GPa)	408.88	394.84	366[24] 369[21]

Table 3: *Direct Γ - Γ and indirect (Γ -X) band gaps for Zincblende InN, BN, and their alloy $B_xIn_{1-x}N$*

Composition	LDA		GGA	
	$E_{\Gamma-\Gamma}$	$E_{\Gamma-X}$	$E_{\Gamma-\Gamma}$	$E_{\Gamma-X}$
InN	0.0000	2.7000	0.0000	2.9200
$B_{0.25}In_{0.75}N$	0.0526	3.1660	0.0141	3.1905
$B_{0.5}In_{0.5}N$	0.8645	3.5625	0.9568	3.4615
$B_{0.75}In_{0.25}N$	3.0025	5.4615	3.0670	5.235
BN	7.5000	4.2101	8.4615	4.4904

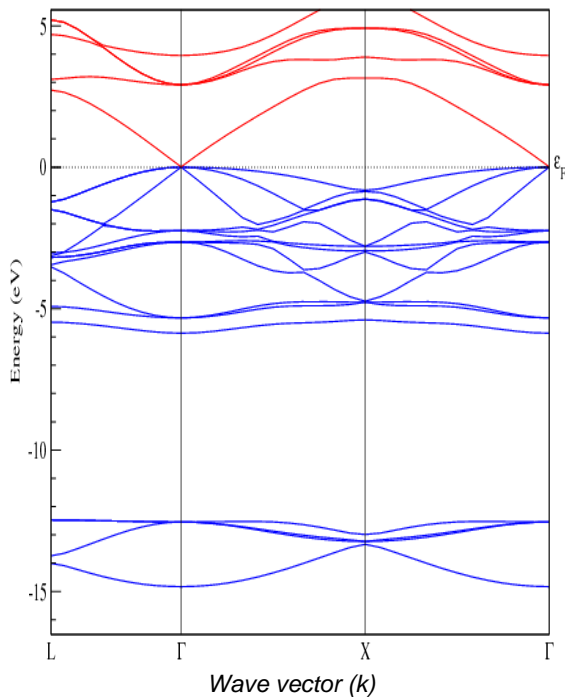


Fig. 3.3: The band structure of $B_{0.25}In_{0.75}N$ within (DFT-LDA). Direct Band gap is 0.0526 eV

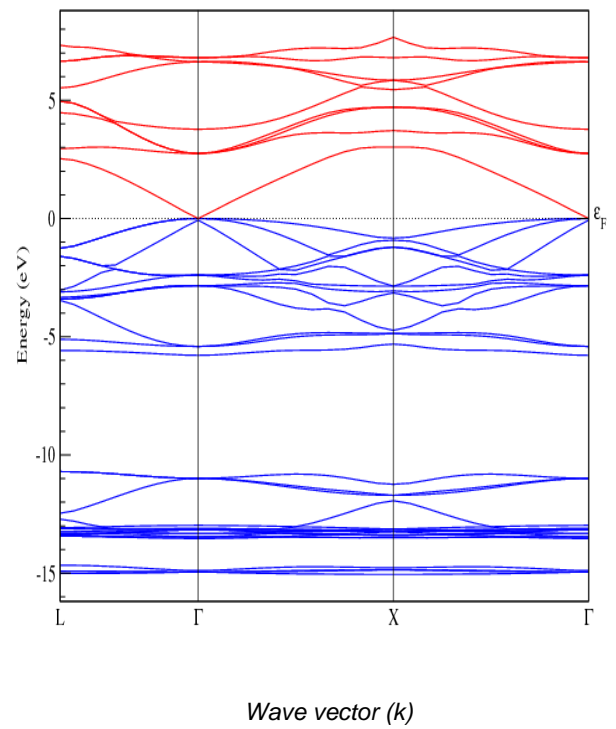


Fig. 3.4: The band structure of $B_{0.25}In_{0.75}N$ within (DFT-GGA). Direct Band gap is 0.0141 eV

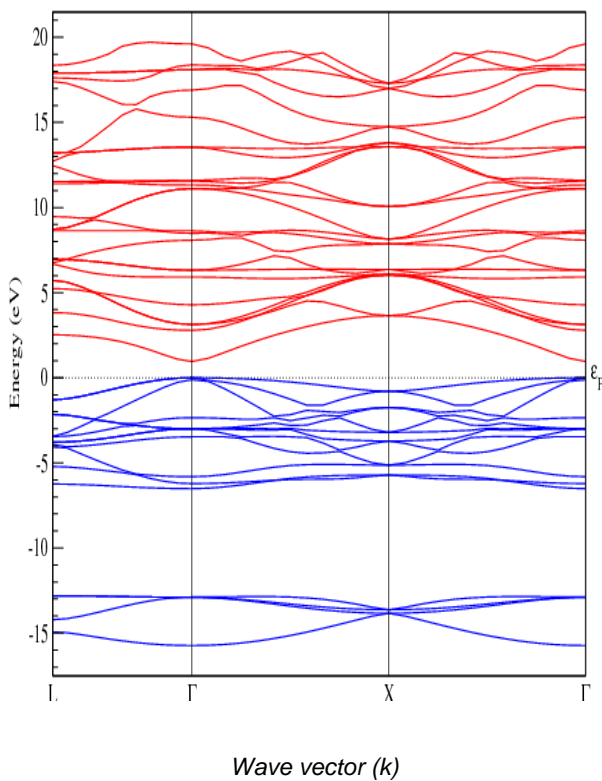


Figure 3.5: The band structure of $B_{0.5}In_{0.5}N$ within (DFT-LDA). Direct Band gap is 0.8645 eV

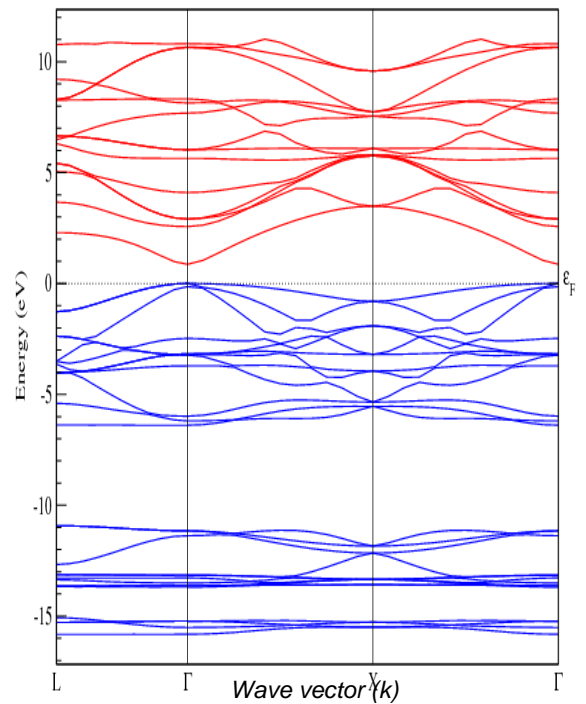


Figure 3.6: The band structure of $B_{0.5}In_{0.5}N$ within (DFT-GGA). Direct Band gap is 0.9568 eV

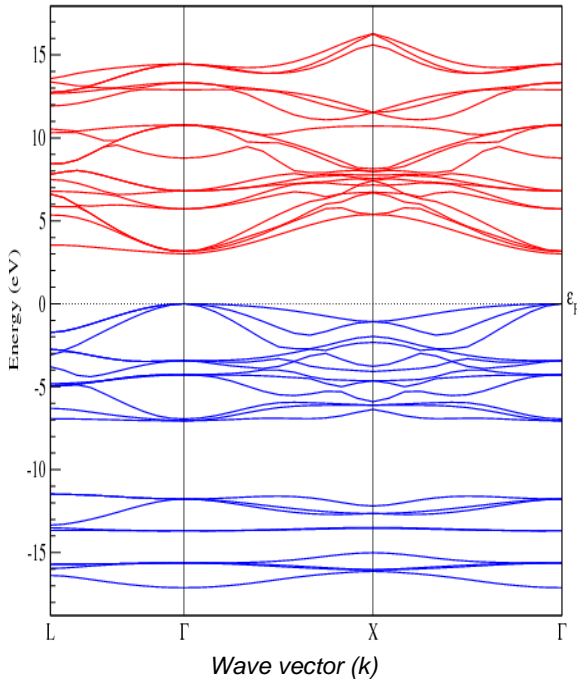


Figure 3.7: The band structure of $B_{0.75}In_{0.25}N$ within (DFT-LDA). Direct Band gap is 3.0025 eV

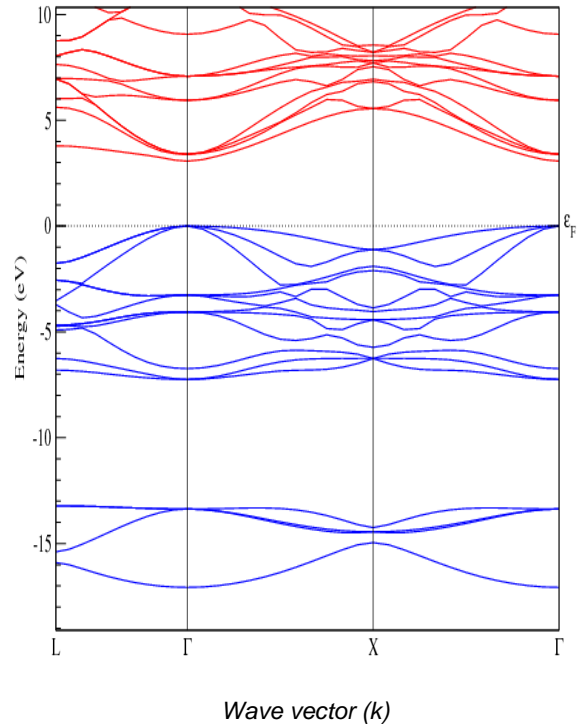


Figure 3.8: The band structure of $B_{0.75}In_{0.25}N$ within (DFT-LDA). Direct Band gap is 3.0670 eV

The variation of the direct $E_{\Gamma-\Gamma}$ and indirect $E_{\Gamma-X}$ band gaps against alloy composition is given in figures 3.9 and 3.10. A crossover between the direct and indirect band gaps is allocated at a concentration of 0.84. Through figure 4, we note that the fundamental gap $E_{\Gamma-\Gamma}$ increases according to the concentration and fall in good term with the evaluation from the lattice constant which decreases when the concentration increases. The total bowing parameter is calculated by fitting the non linear variation of the calculated direct and indirect band gaps in terms of concentration with polynomial function. The results are shown in fig. 5 and obey the following variations:

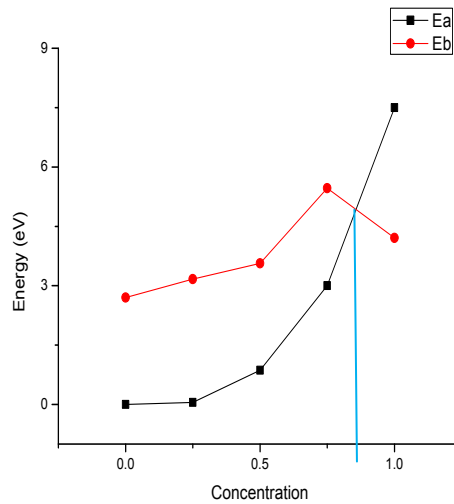


Figure 3.9: Concentration dependence of the direct (Γ - Γ) and indirect (Γ -X) band gaps within DFT-LDA where E_a is direct (Γ - Γ) and E_b is indirect (Γ -X) band gaps in $B_xIn_{1-x}N$ alloys

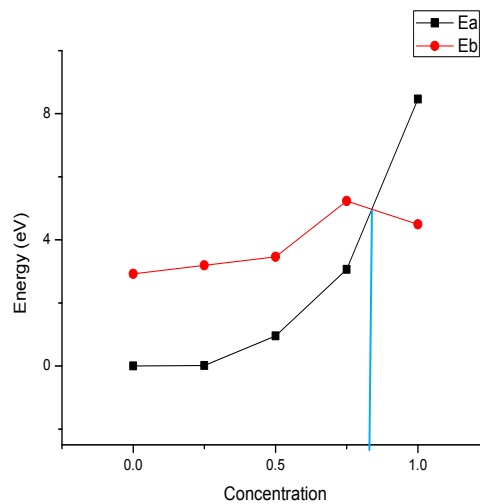


Figure 3.10: Concentration dependence of the direct (Γ - Γ) and indirect (Γ -X) band gaps within DFT-GGA where E_a is direct (Γ - Γ) and E_b is indirect (Γ -X) band gaps in $B_xIn_{1-x}N$ alloys

4.0 CONCLUSION

In this work, the electronic properties of the ternary alloys $B_xIn_{1-x}N$ have been considered in zincblende phase defined by their equilibrium lattice constants. The Pseudopotential method (which is based on the density functional theory (DFT) in the local density approximation (LDA) and the generalized gradient approximation (GGA) have been employed to determine the electronic band structure.

The energy band gap, the bowings of the lattice constant and the bulk modulus were investigated. The alloy $B_xIn_{1-x}N$ for the composition $x = 0.75$ was predicted

to be a wide gap semiconductor and hence, may be a good material for optoelectronic industry. The results show a strong dependence of the band gap bowing factor on the composition x of Boron.

References

- [1]. H.Kawnishi, T. Honda, *Photonics Based on Wavelength Integration and Manipulation*, pp. 19-24 (2005)
- [2]. Yen- Kuang Kuo, Han-Yi Chu, Sheng- Horng Yen, Bo- Tiing Liou and Mei- Ling Chen, *Optic. Communic.*, 280, (2007), 153.
- [3]. X. Gonze, et al., *Computer Phys. Commun.* 180, 2582 (2009).
- [4]. X. Gonze, et al., *Z. Kristallogr.* 220, 558 (2005).
- [5]. N. Trouiller, J. L. Martins, *phys. Rev.B*, 43,(1990), 1993
- [6]. J. P. Perdew, Y. Wang, *phys. Rev. B* 43, 13244 (1992)
- [7]. D. M. Ceperley, B. J. Alder, *phys. Rev. let.* 45, (1980), 566
- [8]. H. J. Monkhorst, J. D. Pack, *phys. Rev. B* 140,(1976) A 1333
- [9]. Larach S., Shrader R.E. and Stocker C. F. (1957). Anomalous Variation of Band Gap with Composition in Zinc Sulfo- and Seleno-Tellurides. *Phys. Rev.* 108, 587 *Phys. Rev.* 108, 587–589.
- [10]. Ebina A., Yamamoto M., Takahashi T., (1972). Reflectivity of $ZnSe_xTe_{1-x}$ Single Crystals. *Phys. Rev. B* 6, 3786–3791.
- [11]. De Caro L., Giannini C., Tapfer L., Schonherr H.-P., Daweritz L. and Ploog K.H. (1998). Validity of Vegard's rule for the lattice parameter and the stiffness elastic constant ratios of the AlGaAs ternary compound. *Solid State Communications*, Vol. 108, No. 8, pp. 599 – 603.
- [12]. Rashkeev S.N., Lambrecht W.R.L. (2001) Second-harmonic generation of I-III-VI₂ chalcopyrite semiconductors: Effects of chemical substitutions. *Phys. Rev. B* 63, 165212-165223.
- [13]. El Haj Hassan F. and Akbarzadeh H., (2005). First-principles investigation of BN_xP_{1-x} , BN_xAs_{1-x} and BP_xAs_{1-x} ternary alloys. *Mater. Sci. Eng. B* 121, 170–177.
- [14]. Dridi Z., Bouhafs B. and Ruterana P., (2005). First-principles study of cubic $Al_xGa_{1-x}N$ alloys. *Comput. Mater. Sci.* 33, 136,136-140.
- [15]. Zpeedeh B. D. F. (2008). First Principle Electronic Structure Calculations of Ternary alloys. BN_xP_{1-x} and $Ga_xB_{1-x}N$ in zinc blende structure. Master of Science in physics An-Najah National University, Nablus –Palestine.
- [16]. K. Kim, W. R. Lambrecht and B. Segall, *Phys. Rev.*, B, 53, (1996), 16 310.
- [17]. A. Trampert, O. Brandt and K. H. Ploog, J. I. Pankove and Moustakas, *Semiconductor and Semimetals.*, 50 ,(1998).
- [18]. M. B. Kanoun, A. E. Merad, G. Merad, J. Cebert, H. Aourag, *Solid-State Electronics.*, 48, (2004), 1601.
- [19]. M. E. Sherwin and T. J. Drummond, *J. Appl. Phys.*, 69, (1991), 842.
- [20]. V. A. Pesin, *Sverktverd. Mater.*, 6, (1980), 5.
- [21]. Knittle, R. M. Wentzcovitch, R. Jeanloz and M and L. Cohen, *Nature (London)*, 337, (1989), 349.

- [22]. S. Fahy, Phys. Rev., B, 51, (1995), 12873.
- [23]. R. M. Wentzcovitch, K. J. Chang, and M. L. Cohen, Phys. Rev., B, 34, (1986), 1071.
- [24]. P.E. Van Camp, V. E. Van Doren and J. T. Devreese, Phys. Rev., B, 41, (1990), 1598.
- [25]. P. Hohenberg and W. John, Phys, Rev. 136, B 864 (1964)
- [26]. W. Kohn and L. J. Sham, Phys. Rev. 140, A1133 (1965)
- [27]. F.D. Murnaghan, Proc Natl Acad Sci U.S.A., 30, 244 (1944)